

Unravelling the Different Reaction Pathways for Low Temperature CO Oxidation on Pt/CeO₂ and Pt/Al₂O₃ by Spatially Resolved Structure-Activity Correlations

Andreas M. Gänzler,^a Maria Casapu,^a Dmitry E. Doronkin,^{a,b} Florian Maurer,^a Patrick Lott,^a Pieter Glatzel,^c Martin Votsmeier,^d Olaf Deutschmann^{a,b} and Jan-Dierk Grunwaldt^{*,a,b}

[a] Institute for Chemical Technology and Polymer Chemistry (ITCP), Karlsruhe Institute of Technology (KIT), Engesserstraße 20, 76131 Karlsruhe (Germany)

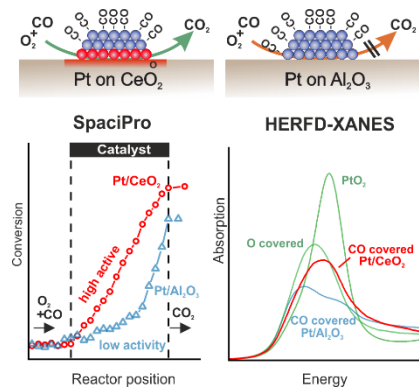
[b] Institute of Catalysis Research and Technology (IKFT), Karlsruhe Institute of Technology (KIT), Hermann-von-Helmholtz-Platz 1, 76344 Eggenstein-Leopoldshafen (Germany)

[c] ESRF – The European Synchrotron, 71 Avenue des Martyrs, 38000 Grenoble (France)

[d] Umicore AG & Co. KG, Rodenbacher Chaussee 4, 63457 Hanau (Germany)

KEYWORDS: CO oxidation, platinum-ceria, interface, HERFD-XANES, spatially resolved operando spectroscopy

ABSTRACT: Spatially resolved *operando* HERFD-XANES (high energy resolution fluorescence detected X-ray absorption near edge structure) complemented by CO concentration gradient profiles along the catalyst bed (SpaciPro) were used to identify the dominant reaction paths for the low and high temperature CO oxidation on Pt/CeO₂ and Pt/Al₂O₃. At low temperatures, features associated to CO adsorption on Pt were found for both catalysts. During the oxidation reaction light-off, the evolution of the spectral and catalytic profile diverged along the catalyst bed. The CO-oxidation rate was high on Pt/CeO₂ from the beginning of the catalyst bed with CO being adsorbed on Pt, whereas low CO-conversion due to strong CO-poisoning was found on Pt/Al₂O₃. This correlation of the CO concentration gradient with unique insight by HERFD-XANES gave direct proof of the crucial contribution of the Pt-CeO₂ perimeter sites overcoming the CO self-inhibition effect at low temperatures.



For many chemical and physical applications the interface between a metal oxide and a noble metal is critical for high performance, e.g. in photocatalytic and photovoltaic devices,¹ sensors² and heterogeneous catalysts.³⁻⁷ In the latter case, understanding, manipulating and controlling the synergy between reducible oxide supports like ceria and catalytically active metal components promises a substantial improvement of today's catalytic materials. This is particularly important for processes which rely on expensive noble metals, e.g. platinum, in exhaust gas abatement commonly applied as small nanoparticles (NPs). Important insight has advanced the field in the past years and has led to speculations with respect to the origin of the beneficial nature. For example,

- electron transfer from oxide support to the noble metal interface,⁸⁻⁹

- oxygen transfer from ceria to noble metal NPs¹⁰⁻¹¹ and
- stabilization of high noble metal dispersion or even single sites as well as their capability to re-disperse noble metal NPs under oxidizing conditions.¹²⁻¹⁴

In particular, ceria-based catalysts have become outstanding candidates for the removal of automotive exhaust gas pollutants in three-way catalysts, diesel oxidation catalysts and those for VOC-removal.¹⁵⁻¹⁷ In addition, the potential of Pt/CeO₂ catalysts for low-temperature CO oxidation has been highlighted in recent studies, with the noble metal-support interface claimed as a key parameter.^{11, 14, 18} However, the underlying working principle regarding the role of the noble metal, of the support and of the Pt/CeO₂ interface as well as the nature of Pt, i.e. particles, clusters or single sites, is still strongly debated.¹⁹⁻²³ Furthermore,

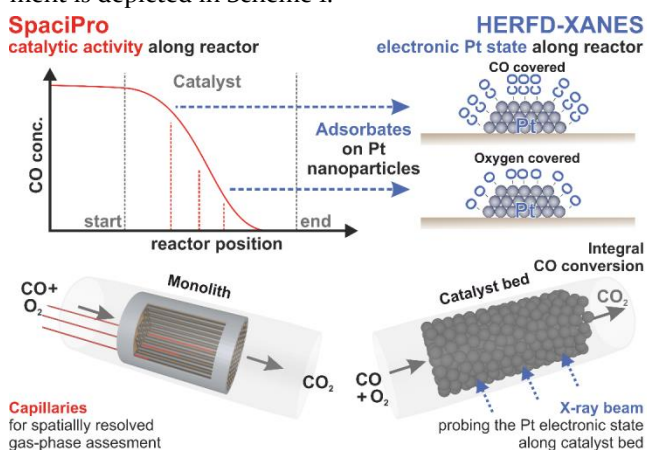
the evolution of the noble metal sites under reaction conditions (i.e. *operando*) and, especially, their interaction with CO and O₂ are hardly reported in literature. The latter aspect is particularly important considering that Pt based catalysts commonly suffer of a prominent issue: “CO self-poisoning” of the noble metal surface.²⁴⁻²⁶ Due to strong CO adsorption, Pt sites are blocked and not accessible for oxygen adsorption. This substantially diminishes the catalytic activity at low-temperatures.²⁷⁻²⁹ Additionally, to consolidate and understand a reaction mechanism, such structural changes that evolve under transient reaction conditions need to be followed in a spatially (along the catalyst bed) and time (during start-up, operation and the entire catalyst lifetime) resolved manner,³⁰⁻³² and preferentially correlated with locally assessed activity data.³³⁻³⁴

For *operando* studies, needed for a robust correlation between catalytic activity and catalyst structure, X-ray based methods like X-ray absorption spectroscopy (XAS) are attractive.^{30-31, 35} Here, we use the more advanced photon-in/-out-technique *high energy resolution fluorescence detected X-ray absorption near edge structure* (HERFD-XANES),³⁶⁻³⁸ which is even more powerful, since it both employs highly penetrating X-rays and provides in-depth information on the noble metal atomic and electronic structure.³⁹⁻⁴¹ HERFD-XANES can recognize the impact of adsorbates on the noble metal electronic structure, and it is thus able to probe CO adsorption on Pt.⁴² This approach thus allows the study of CO adsorption *operando* directly from the perspective of the Pt component, as compared to IR-based methods, which are generally used to approach such questions. The latter characterizes the electronic structure of Pt species indirectly by studying changes in the CO stretching frequency.⁴³⁻⁴⁴ Therefore, the adsorption of CO is a prerequisite, which prevents the acquisition of information on short-lived adsorbed CO species during CO oxidation. Hence, Pt species not suitable for CO adsorption are practically hidden from the experimentalist. Although HERFD-XANES has been demonstrated powerful for gathering information on adsorbates,⁴⁵⁻⁴⁶ there are still only few studies which use it as *operando* technique to elucidate reaction mechanisms in heterogeneous catalysis.^{28, 38, 47-49}

Apart from further developing *operando* techniques, recording them in a spatially resolved manner is important as the concentration and temperature strongly change along a catalyst bed and just measuring at one location in the device, i.e. the reactor, is not sufficient. In fact, recent spectroscopic studies underline the need and potential of a spatially resolved assessment of the catalyst bed or catalytic reactor for the establishment of a robust mechanistic understanding, as well as to elucidate the catalytically active component.^{30, 50-51} These studies generally aim at unraveling atomic-scale properties like the structure of noble metal NPs, their oxidation state or adsorbate coverage along the catalyst bed. This allows to elaborate on gradients, how they evolve and how they are related to macro-scale processes like temperature hot-spots, heat transfer

and mass transport.^{32, 52-55} Their information becomes particularly powerful when correlated to spatially resolved catalytic activity data, obtained e.g. by spatial profiling of the gas phase using a thin capillary coupled with a sensitive gas analysis (SpaciPro).^{33, 56-60} This approach appears ideal to probe structural variations inside reactors where gradients evolve, notably due to poisoning by surface adsorbates, such as CO, and due to the reaction.

In the present study we thus evaluate the different CO oxidation mechanisms over Pt/Al₂O₃- and Pt/CeO₂-based catalysts by comparing the CO gas phase concentration along the catalyst bed under reaction conditions and by correlating it to the electronic structure of platinum (oxidation state and coverage by CO). In this way, the special role of the Pt-ceria interface for the CO oxidation catalysis is directly probed. For this purpose, a 1wt.%Pt/CeO₂ and a 1wt.%Pt/Al₂O₃ with similar Pt particle size were investigated using the SpaciPro technique for determining the conversion profiles and *operando* XAS, including more advanced HERFD-XANES to identify the structure of catalytically active CO covered Pt NPs in Pt/CeO₂ and to elaborate on their mechanistic role for low-temperature CO oxidation. The catalysts were coated as a layer of 50-100 μm on cordierite honeycombs for concentration profiles by SpaciPro and a sieve fraction of 100-200 μm in a 1.5 mm thick microreactor was used for spectroscopic studies. The experiments were correlated via integral mass spectrometric information. The central idea and course of the experiment is depicted in Scheme 1.



Scheme 1. Correlating spatially resolved gas-phase concentration profiles (SpaciPro) with spatially resolved information on Pt electronic state and adsorbates (HERFD-XANES) via integral catalytic activity data.

Pt/Al₂O₃ and Pt/CeO₂ catalysts were prepared by incipient wetness impregnation. In a first step, γ-alumina (Puralox, SASOL) and ceria (MEL Chemicals) were pretreated in air at 700 °C for 5 h. The resulting surface area was 165 m²/g for Al₂O₃ and 30 m²/g for CeO₂. The Pt precursor material, tetraamineplatinum(II)nitrate (STREM Chemicals), was dissolved in water and added dropwise to the support. The resulting powder was dried over night at 70 °C and calcined

at 500 °C for 5 h in static air. The Pt loading was confirmed by inductively coupled plasma optical emission spectrometry (ICP-OES) using an OPTIMA 4300 DV spectrometer (PerkinElmer) at the Institute for Applied Materials (KIT). N₂ physisorption (BELSORP-mini II, Rubotherm) was conducted at -196 °C to estimate the specific surface area according to the Brunauer-Emmett-Teller (BET) method.⁶¹ High angle annular dark field scanning transmission electron microscopy (HAADF-STEM) images were acquired by probing pre-reduced catalyst samples (2 % H₂/N₂, 2 h at 400 °C) with a FEI OSIRIS microscope operated at 200 kV at the Laboratory for Electron Microscopy (KIT). For Pt particle size distributions, the average diameter of >1000 NPs was evaluated assuming an elliptical shape. As the study focusses on the origin of the outstanding activity of Pt/CeO₂, they have been studied after a reducing pre-treatment, for which highest catalytic activity was observed,^{14, 62-63} with Pt present as small reduced Pt NPs confirmed.^{14, 64}

For SpaciPro experiments, the catalyst powder was coated on cordierite monoliths (cell density: 400 cpsi, 19 mm x 30 mm), and tested in plug-flow quartz tube reactors (WHSV of 60 000 L^{*}g_{Pt}⁻¹h⁻¹). Gases were dosed using mass flow controllers (Bronkhorst). The product gases were sampled with a quartz glass capillary (OD = 170 μm) and analyzed using a sensitive mass spectrometer (HPR-20, Hiden Analytics). The impact of such a physical probe within the catalyst has been discussed earlier.⁵⁷ The catalysts were pre-reduced prior to the catalytic measurement (2% H₂/N₂, 2h at 400 °C). The CO concentration was probed along the monolithic reactor in a so-called lean (large oxygen excess) CO oxidation mixture (1000 ppm CO, 10 % O₂, N₂) at various temperatures (see ESI). For the comparison, the focus is laid on data obtained at ~50 % CO conversion.

Operando HERFD-XANES experiments were conducted at ESRF (Grenoble, France) at beamline ID26. The energy of the incident monochromatic X-rays was selected, using a cryogenically cooled Si (311) double crystal monochromator. The X-ray beam footprint on the sample was 700 μm horizontal * 100 μm vertical. Five spherically bent (R=1 m) Ge (660) analyzer crystals (Rowland geometry) were utilized to select the fluorescence at the maximum of the Pt-L_α emission line (9442 eV), which was recorded with an avalanche photodiode detector, while the incident energy was scanned around Pt-L₃ absorption edge (11564 eV). As a change of the Pt chemical state has been observed previously upon exposure to an X-ray beam with high photon flux, we used a (311) monochromator (which results in higher energy resolution at the expense of photon flux as compared to the Si(111) reflection) and beam absorber (800 μm Al-foil attenuating 97 % of X-ray photons at 11563 eV) to a point where no changes could be observed upon irradiation of the samples (tested by continuously recording ~5 s quick XANES spectra). The catalysts (sieved fraction 100-200 μm) were loaded in quartz glass capillaries (1.5 mm outer diameter, 10 μm wall thickness) heated by a hot air

gas blower.⁶⁵ Gases were supplied using mass-flow controllers (Bronkhorst) at a WHSV of 60 000 L^{*}g_{Pt}⁻¹h⁻¹. The reaction products were monitored with a quadrupole mass spectrometer (Pfeiffer Vacuum, OmniStar GSD 320) and an online FTIR gas analyzer (MKS, Multigas 2030). The catalysts were pre-reduced prior to the catalytic measurement (2 % H₂/He, 30 min at 400 °C). Afterwards the lean CO reaction mixture (1000 ppm CO, 10 % O₂, He) was applied at room temperature and the temperature was increased stepwise. At each step, HERFD-XANES spectra were obtained at three positions along the catalyst bed (start, middle, end). Several spectra were merged to increase the data quality and filtered (Savitzky-Golay) before normalization (pre-edge normalization range: -150 eV to -50 eV; post edge normalization range: 150 eV to 400 eV). The data were quantitatively evaluated by linear combination fitting (fitting range: 11560 eV and 11575 eV) using spectra representing Pt in a completely oxidized and surface oxidized state, as well as reduced Pt NPs in He and CO/He atmosphere (see Figure 3a-b). The state ascribed as “surface oxidized” is represented by the spectrum obtained at the end of the catalyst bed of Pt/Al₂O₃ at 150 °C under CO oxidation conditions (full CO conversion)

HAADF-STEM images (Figure 1) uncovered very small Pt NPs for both catalysts, 1wt.%Pt/Al₂O₃ and 1wt.%Pt/CeO₂, after reductive treatment of the catalyst, with narrow size distribution (more than 99 % of the particles below 1.5 nm) and mean Pt-particle diameters of 0.8 nm and 0.9 nm for Pt/Al₂O₃ and Pt/CeO₂ respectively. Hence, they are ideal model catalysts for comparing their catalytic activity and their structural evolution under reaction conditions as well as for identifying the descriptors responsible for the superior kinetics of the ceria based catalyst.

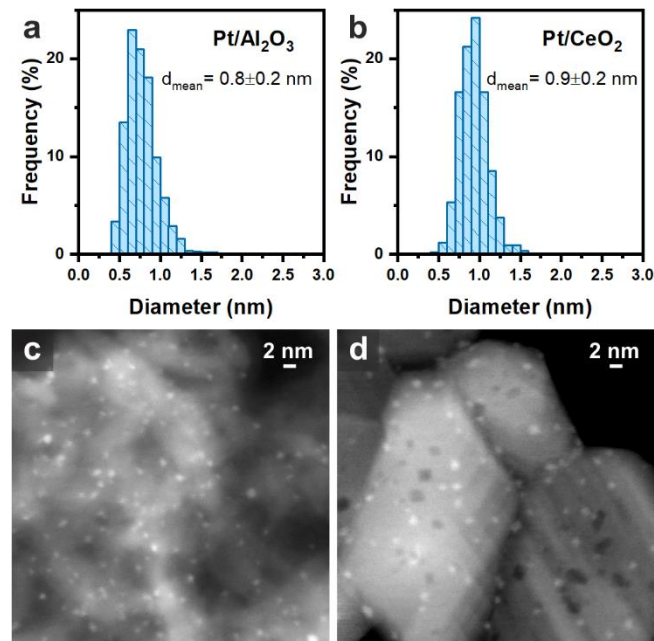


Figure 1. Particle size distribution of a) Pt/Al₂O₃ and b) Pt/CeO₂ together with corresponding HAADF-STEM images of c) Pt/Al₂O₃ and d) Pt/CeO₂.

The CO conversion profiles recorded along the central channel of the two monolithic catalysts by SpaciPro during CO oxidation are shown in Figure 2a (increase of the temperature leads to a smaller oxidation zone, cf. further profiles in Figure S1). The profiles were obtained at temperatures of ~50 % overall CO conversion (denoted T₅₀ or light-off temperature) of the respective catalysts (95 °C for Pt/CeO₂, 140 °C for Pt/Al₂O₃) after a reductive pre-conditioning step. The superior integral CO oxidation activity for Pt/CeO₂ compared to Pt/Al₂O₃ is in a good agreement with previous studies.^{14, 18}

As illustrated in Figure 2a, prominent differences in the concentration profiles along the monolith channels are found for the two catalysts. For Pt/CeO₂, CO was converted at a similar rate at all positions along the catalyst bed, with a linearly increasing CO conversion corresponding to a reaction order of zero (Figure 2b). In contrast, a negative reaction order with respect to CO was observed over Pt/Al₂O₃.¹⁸ Note that there is some scattering and a rather small CO partial pressure regime. According to a Langmuir-Hinshelwood model a maximum slope of -1 would be expected in case of strong CO-poisoning. Hence, after two thirds of the catalyst about 10 % CO conversion were observed for Pt/Al₂O₃ at 140 °C, whereas for Pt/CeO₂ 30 % CO conversion was achieved at the same position of the catalyst bed already at 95 °C. This reflects the impact of the CO concentration on all Pt surface sites in the case of Pt/Al₂O₃ in contrast to Pt/CeO₂.

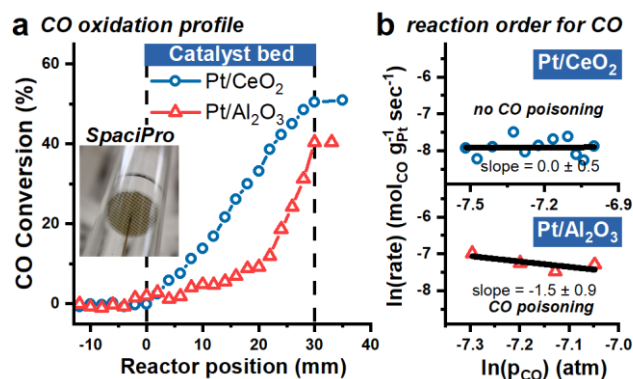


Figure 2. a) CO conversion along pre-reduced Pt/CeO₂ (blue circles) and Pt/Al₂O₃ (red triangles) coated monoliths at ~50 % integral CO conversion (1000 ppm CO, 10 % O₂, N₂). b) Linear regression of logarithmic plot of the CO oxidation rate as function of the CO partial pressure along the catalyst bed. The slope indicates the reaction order of the CO oxidation rate.

In order to probe the structure of Pt and CO coverage on Pt along the reactor, HERFD-XANES at the Pt-L₃ edge was applied. Spatially resolved data were obtained by moving the catalyst bed in the focused X-ray beam. Pt-L₃ edge HERFD-XANES spectra contain additional information on

the adsorption of CO on Pt in comparison to conventional XANES.⁴² The attractive opportunities to probe CO on Pt and its oxidation state are illustrated in Figure 3a where CO was dosed to the pre-reduced Pt/Al₂O₃ and Pt/CeO₂ catalysts. After reduction at 400 °C in H₂ the spectra obtained at room temperature revealed the well-known white-line profile (~11564 eV) of reduced Pt.^{42, 66} Upon dosing 1000 ppm CO in He to the reduced catalyst, the absorption intensity increased at higher energies (~11569 eV) and a pronounced double peak feature evolved in the case of Pt/Al₂O₃, which was earlier attributed to the atop adsorption geometry of CO on Pt.⁴² In contrast, in the case of Pt/CeO₂ a shoulder was recognized at 11569 eV similar as in the case of Pt/TiO₂.⁶⁶ This feature also originates from CO adsorption and was previously assigned to CO adsorbed to Pt in a bridged mode, based on calculations for unsupported Pt₆ cluster with a CO molecule adsorbed on different Pt sites.⁴² The CO-band may also be altered by interaction of Pt with the support. Upon exposure to oxygen the white-line intensity increased, and the spectrum was dominated by a feature at around 11567 eV (Figure 3b). Much higher absorption was observed for oxidized Pt NPs resulting in a narrow peak at 11568 eV (Figure 3b).

In a next step, *operando* HERFD-XANES data were recorded at selected temperatures in a model lean CO oxidation mixture (1000 ppm CO, 10 % O₂, He). At each temperature during the CO oxidation light-off the catalyst bed was probed at start, middle and end position, while the outlet CO concentration was simultaneously monitored. *Operando* HERFD-XANES data are presented for Pt/Al₂O₃ and Pt/CeO₂ in Figure 4a-f (full data set in Figure S2-S5). The data were furthermore quantitatively evaluated with linear combination fitting (LCF, Figure 5, further information Figure S6+S7), using spectra representing Pt in a bulk oxidized and surface oxidized states, as well as reduced Pt NPs in He and CO/He atmosphere (Figure 3a+b). The contributions of the references for CO and oxygen covered Pt NPs to the fit of the experimental data are presented for Pt/Al₂O₃ and Pt/CeO₂ in Figure 5 (indicated as colored circles) and compared to their respective CO oxidation activity (indicated as grey triangles). Upon addition of oxygen to the reaction atmosphere at room temperature, Pt partially oxidized as indicated by an increase of the white-line intensity at higher energies (~11568 eV), particularly in the case of Pt/CeO₂ (Figure 3, further details in Figure S4).

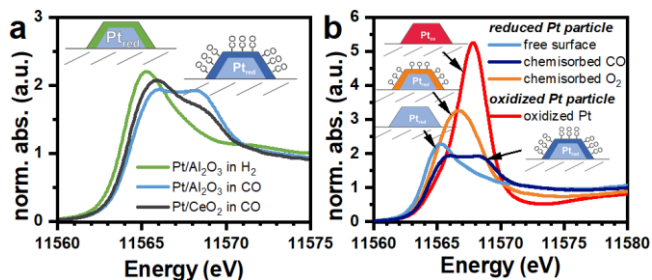


Figure 3. Variation of Pt L₃ HERFD-XANES spectra by CO adsorption a) CO covered and CO free reduced Pt NPs in Pt/Al₂O₃ and Pt/CeO₂ and b) reference states: reduced Pt NPs with free, CO covered and oxygen covered surface, as well as oxidized Pt NPs. Low absorption intensity with a broad feature indicates adsorption of CO on reduced Pt, while high absorption intensity results from oxidation of Pt.

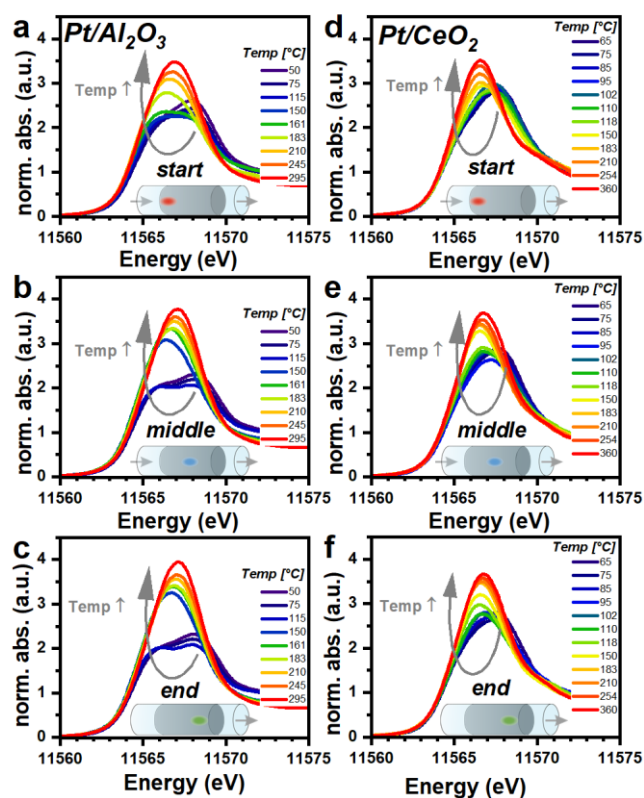


Figure 4. Operando Pt-L₃ HERFD-XANES obtained at the start, middle and end of the catalyst bed of Pt/Al₂O₃ (a-c) and Pt/CeO₂ (d-f) during CO oxidation (1000 ppm CO, 10 % O₂, He) at various temperature plateaus.

During heating in the CO oxidation mixture, a distinct gradient in CO adsorption along the catalyst bed evolved in the case of Pt/Al₂O₃. At low temperatures (below 115 °C), this catalyst showed low CO conversion (Figure 5, <15 % CO conversion) while the LCF analysis of the HERFD-XANES data revealed CO adsorption on Pt NPs at all catalyst bed positions, underlining a strong poisoning effect by CO. In fact, the initial partial oxidation of Pt was reversed

within this stage, and the white-line double feature characteristic for CO adsorption on Pt was observed for all positions at 115 °C (Figure 4). This reduction of Pt appears to play an important role for the catalyst activity, as it just precedes the transition from the low to the high active regime. The same Pt oxidation state evolution was also identified with conventional time-resolved XAS measurements presented in Figure S8.

At 150 °C full CO conversion was observed for Pt/Al₂O₃ behind the reactor. However, while at the beginning of the catalyst bed Pt NPs were still covered by CO (Figure 5a), they were covered by oxygen at the middle and end position (Figure 5b). Due to significant CO conversion at positions closer to the inlet side, the amount of CO was substantially diminished for the rest of the catalyst bed. Therefore, oxygen could readily access the Pt surface, which could cause surface oxidation and, at higher temperature, also bulk oxidation of Pt particles (see also Figure S6 for further details of the LCF analysis). At the start of the catalyst bed, the same evolution was also observed above 160 °C.

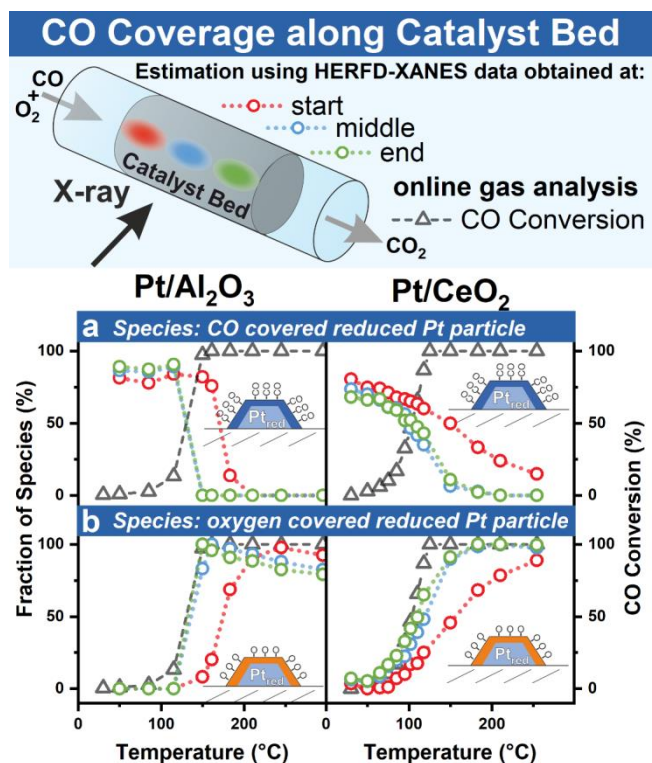
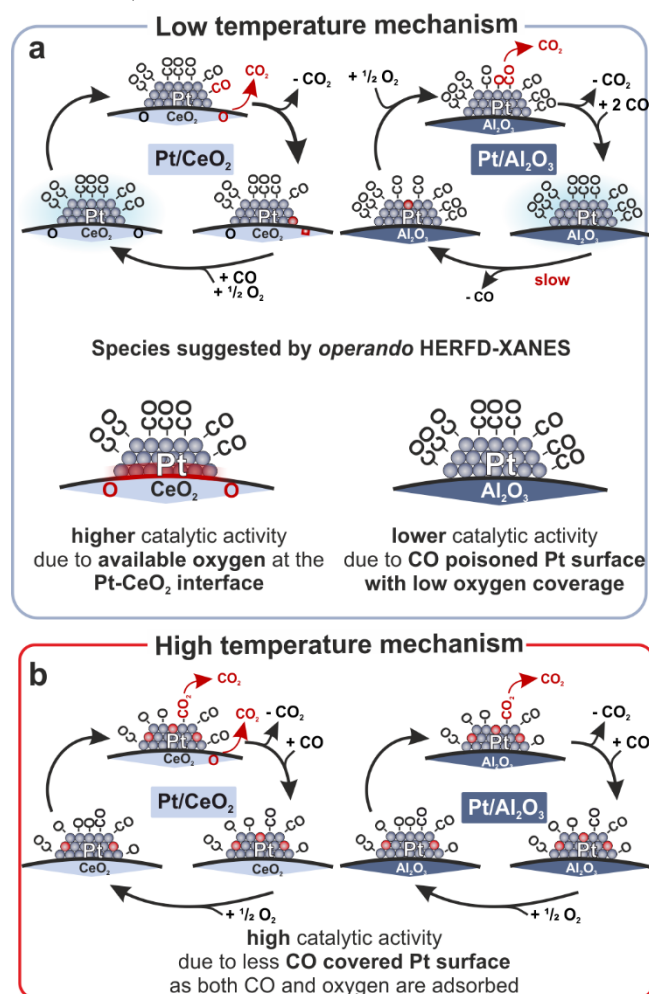


Figure 5. Evaluation of a) CO and b) oxygen coverage of Pt NPs by linear combination fitting (LCF) analysis of Pt-L₃ edge operando HERFD-XANES spectra obtained on Pt/Al₂O₃ and Pt/CeO₂ during CO oxidation. The contribution to the LCF for each component along with conversion of CO is presented for Pt/Al₂O₃ (left) and Pt/CeO₂ (right) along the catalyst bed (start in red, middle in blue and end position in green). The contribution of completely oxidized Pt and Pt NPs with a free surface are shown in Figure S8.

For Pt/CeO₂ the LCF analysis of the HERFD-XANES data revealed a strikingly different evolution (Figure 5). CO was already significantly converted at lower temperature (~100 °C) with less pronounced gradients in the Pt state along the catalyst bed. In fact, also at high CO conversion (>80 %) Pt NPs on ceria were still substantially covered by CO (>30 %) at downstream positions (Figure 5) compared to Pt/Al₂O₃. Only above 110 °C the white-line intensity started to increase at the end of the catalyst bed. Since in the front part most of CO was converted, Pt NPs were oxidized at the end. For this case, the CO oxidation rate was found to be independent of the position along the catalyst bed for Pt/CeO₂ (Figure 2). As Pt NPs were still prominently covered by CO, the Pt-ceria interface probably enabled CO oxidation. The same behavior was found at the middle at temperatures above 120 °C (>85 % conversion) and at the start of the catalyst bed above 150 °C (full CO conversion).



Scheme 2. Dominant CO oxidation reaction pathways for Pt/CeO₂ and Pt/Al₂O₃ at a) low temperature and b) high temperature.

In summary, SpaciPro unraveled a homogeneous and equally high catalytic activity along the catalyst bed for Pt/CeO₂ at low temperatures (Figure 2). In the light of the HERFD-XANES characterization of the Pt component (Figures 4 and 5), the origin of the superior catalytic properties can be assigned to CO covered Pt NPs. Although CO covered, these Pt NPs on ceria are able to oxidize CO despite of CO-poisoning of the Pt particle, by exploiting the oxygen species at the noble metal-ceria interface. In contrast, for the Pt/Al₂O₃ catalyst, partial desorption of CO is a prerequisite to allow the access of oxygen to Pt sites for the onset of CO oxidation (Figure 5). These two different reaction pathways are also reflected by the SpaciPro data (Figure 2), which show the participation of the entire catalyst bed for Pt/CeO₂ and of mainly the end of catalyst bed for Pt/Al₂O₃ catalyst (including a negative reaction order for CO) to achieve about 50 % CO conversion.

This difference explains the substantially lower light-off temperature over Pt/CeO₂ and the resulting mechanism is illustrated in Scheme 2a. In addition, the altered reaction pathways for Pt/CeO₂ and Pt/Al₂O₃ at elevated temperatures are shown in Scheme 2b. At high temperature CO oxidation is efficiently catalyzed on the Pt surface for both catalyst systems. However, when the Pt surface gets covered by CO at lower temperature and the oxidation reaction on the Pt surface is inhibited, the Pt-CeO₂ interface still provides oxygen from the support to the CO covered surface.

In conclusion, complementary structural (*operando* HERFD-XANES) and catalytic activity data (SpaciPro) were obtained in a spatially resolved manner for Pt/CeO₂ and Pt/Al₂O₃. *Operando* HERFD-XANES provided additional information on the adsorbed species compared to conventional XAS. The results thus allowed to thoroughly probe the different reaction paths for CO oxidation on these academically and industrially relevant catalysts. Although the spectroscopic data unraveled that Pt particles are CO covered at low temperature on both catalysts, no CO inhibition zone could be identified along the Pt/CeO₂ catalyst bed according to the measured CO concentration profile. In contrast, significant CO conversion was observed only at the middle and end of the catalyst bed for Pt/Al₂O₃, in line with the negative reaction order with respect to CO observed by SpaciPro. At low temperature, we conclude that the CO oxidation occurs at the noble metal-support interface with oxygen provided via ceria perimeter sites. These perimeter sites in combination with CO-covered and thus reduced Pt particles (depicted in Figure 2a) are crucial to enable a fast reaction pathway at low temperature. Superior catalytic activity for Pt/CeO₂ is therefore associated to active sites with this unique local chemical arrangement. The lower CO coverage, derived from the

operando HERFD-XANES spectra collected at high temperatures, indicates that in addition to the low temperature mechanism, the CO oxidation reaction on Pt/CeO₂ presumably follows also the Langmuir-Hinshelwood mechanism, which predominantly occurs on Pt/Al₂O₃.

Hence, the results demonstrate a temperature dependent mechanism for Pt/CeO₂ and highlight the importance of the sites at the perimeter between ceria and pre-reduced Pt NPs for the low temperature CO oxidation. Furthermore, the study emphasizes future application of an advanced characterization toolbox for simultaneously unraveling the structure and catalytic properties of the active species in catalytic reactors. The outcome holds important implications for the atomic- and macro-scale design of catalysts and underlines the importance of hierarchical characterization of catalytic systems with respect to the atomic and macroscale as well as the correlation of structure and activity in a spatiotemporal manner.

ASSOCIATED CONTENT

Supporting Information. Supplementary SpaciPro data (Figure S1), *operando* HERFD-XANES data (Figure S2-S7) and *operando* XAS data (Figure S8)

AUTHOR INFORMATION

Corresponding Author

* grunwaldt@kit.edu

Notes

The authors declare no competing financial interest

ACKNOWLEDGMENT

The authors thank the German Federal Ministry for Economic Affairs and Energy (BMWi: 19U15014B) for financial support of the ORCA project within the DEUFRAKO program and the ESRF for beamtime at beamline ID26 (proposal CH-5122). Azize Ünal and Kyle Karinshak are acknowledged for support during SpaciPro measurements and Deniz Zengel for his help during *operando* HERFD-XANES experiments, as well as Rafal Baran for his support during the beamtime at ID26. We acknowledge SOLEIL for provision of synchrotron radiation facilities and we would like to thank Valérie Briois and Stéphanie Belin for assistance in using beamline "ROCK" (financed by the French National Research Agency (ANR) as part of the "Investissements d'Avenir" program (reference: ANR-10-EQPX-45). Heike Störmer (Laboratory for Electron Microscopy, KIT) is acknowledged for recording HAADF-STEM images of catalyst samples, Angela Deutsch for N₂-physisorption measurements and Thomas Bergfeldt (Institute for Applied Materials, KIT) for elemental analysis.

REFERENCES

(1) Clavero, C. Plasmon-induced hot-electron generation at nanoparticle/metal-oxide interfaces for photovoltaic and photocatalytic devices. *Nature Photonics* **2014**, *8*, 95.

(2) Miller, D. R.; Akbar, S. A.; Morris, P. A. Nanoscale metal oxide-based heterojunctions for gas sensing: A review. *Sensors and Actuators B: Chemical* **2014**, *204*, 250-272.

(3) Campbell, C. T. Ultrathin metal films and particles on oxide surfaces: structural, electronic and chemisorptive properties. *Surf. Sci. Rep.* **1997**, *27* (1), 1-111.

(4) Park, J. Y.; Baker, L. R.; Somorjai, G. A. Role of Hot Electrons and Metal-Oxide Interfaces in Surface Chemistry and Catalytic Reactions. *Chem. Rev.* **2015**, *115* (8), 2781-2817.

(5) Ro, I.; Resasco, J.; Christopher, P. Approaches for Understanding and Controlling Interfacial Effects in Oxide-Supported Metal Catalysts. *ACS Catal.* **2018**, *8* (8), 7368-7387.

(6) Suchorski, Y.; Kozlov, S. M.; Bepalov, I.; Datler, M.; Vogel, D.; Budinska, Z.; Neyman, K. M.; Rupprechter, G. The role of metal/oxide interfaces for long-range metal particle activation during CO oxidation. *Nat. Mater.* **2018**, *17* (6), 519-522.

(7) An, K.; Alayoglu, S.; Musselwhite, N.; Plamthottam, S.; Melae, G.; Lindeman, A. E.; Somorjai, G. A. Enhanced CO Oxidation Rates at the Interface of Mesoporous Oxides and Pt Nanoparticles. *J. Am. Chem. Soc.* **2013**, *135* (44), 16689-16696.

(8) Bruix, A.; Rodriguez, J. A.; Ramirez, P. J.; Senanayake, S. D.; Evans, J.; Park, J. B.; Stacchiola, D.; Liu, P.; Hrbek, J.; Illas, F. A New Type of Strong Metal-Support Interaction and the Production of H₂ through the Transformation of Water on Pt/CeO₂(111) and Pt/CeOx/TiO₂(110) Catalysts. *J. Am. Chem. Soc.* **2012**, *134* (21), 8968-8974.

(9) Wang, Y.-G.; Yoon, Y.; Glezakou, V.-A.; Li, J.; Rousseau, R. The Role of Reducible Oxide-Metal Cluster Charge Transfer in Catalytic Processes: New Insights on the Catalytic Mechanism of CO Oxidation on Au/TiO₂ from ab Initio Molecular Dynamics. *J. Am. Chem. Soc.* **2013**, *135* (29), 10673-10683.

(10) Vayssilov, G. N.; Lykhach, Y.; Migani, A.; Staudt, T.; Petrova, G. P.; Tsud, N.; Skála, T.; Bruix, A.; Illas, F.; Prince, K. C.; Matolín, V.; Neyman, K. M.; Libuda, J. Support nanostructure boosts oxygen transfer to catalytically active platinum nanoparticles. *Nat. Mater.* **2011**, *10* (4), 310-315.

(11) Kopelent, R.; van Bokhoven, J. A.; Szlachetko, J.; Edebeli, J.; Paun, C.; Nachttegaal, M.; Safonova, O. V. Catalytically Active and Spectator Ce³⁺ in Ceria-Supported Metal Catalysts. *Angew. Chem. Int. Ed.* **2015**, *54* (30), 8728-8731.

(12) Nagai, Y.; Hirabayashi, T.; Dohmae, K.; Takagi, N.; Minami, T.; Shinjoh, H.; Matsumoto, S. Sintering inhibition mechanism of platinum supported on ceria-based oxide and Pt-oxide-support interaction. *J. Catal.* **2006**, *242* (1), 103-109.

(13) Bruix, A.; Lykhach, Y.; Matolínová, I.; Neitzel, A.; Skála, T.; Tsud, N.; Vorokhta, M.; Stetsovych, V.; Ševčíková, K.; Mysliveček, J.; Fiala, R.; Václavů, M.; Prince, K. C.; Bruyère, S.; Potin, V.; Illas, F.; Matolín, V.; Libuda, J.; Neyman, K. M. Maximum Noble-Metal Efficiency in Catalytic Materials: Atomically Dispersed Surface Platinum. *Angew. Chem. Int. Ed.* **2014**, *53* (39), 10525-10530.

(14) Gänzler, A. M.; Casapu, M.; Vernoux, P.; Loridant, S.; Cadete Santos Aires, F. J.; Epicier, T.; Betz, B.; Hoyer, R.; Grunwaldt, J.-D. Tuning the Structure of Platinum Particles on Ceria In Situ for Enhancing the Catalytic Performance of Exhaust Gas Catalysts. *Angew. Chem. Int. Ed.* **2017**, *56* (42), 13078-13082.

(15) Nagai, Y.; Dohmae, K.; Ikeda, Y.; Takagi, N.; Tanabe, T.; Hara, N.; Guilera, G.; Pascarelli, S.; Newton, M. A. A.; Kuno, O.; Jiang, H.; Shinjoh, H.; Matsumoto, S. i. In Situ Redispersion of Platinum Autoexhaust Catalysts: An On-Line Approach to Increasing Catalyst Lifetimes? *Angew. Chem. Int. Ed.* **2008**, *47* (48), 9303-9306.

(16) Montini, T.; Melchionna, M.; Monai, M.; Fornasiero, P. Fundamentals and Catalytic Applications of CeO₂-Based Materials. *Chem. Rev.* **2016**, *116* (10), 5987-6041.

(17) Jones, J.; Xiong, H.; DeLaRiva, A. T.; Peterson, E. J.; Pham, H.; Challa, S. R.; Qi, G.; Oh, S.; Wiebenga, M. H.; Pereira Hernández, X. I.; Wang, Y.; Datye, A. K. Thermally stable single-atom platinum-on-ceria catalysts via atom trapping. *Science* **2016**, *353* (6295), 150-154.

- (18) Cargnello, M.; Doan-Nguyen, V. V. T.; Gordon, T. R.; Diaz, R. E.; Stach, E. A.; Gorte, R. J.; Fornasiero, P.; Murray, C. B. Control of Metal Nanocrystal Size Reveals Metal-Support Interface Role for Ceria Catalysts. *Science* **2013**, *341* (6147), 771-773.
- (19) Ke, J.; Zhu, W.; Jiang, Y.; Si, R.; Wang, Y.-J.; Li, S.-C.; Jin, C.; Liu, H.; Song, W.-G.; Yan, C.-H. Strong Local Coordination Structure Effects on Subnanometer PtO_x Clusters over CeO₂ Nanowires Probed by Low-Temperature CO Oxidation. *ACS Catal.* **2015**, *5* (9), 5164-5173.
- (20) Nie, L.; Mei, D.; Xiong, H.; Peng, B.; Ren, Z.; Hernandez, X. I. P.; DeLaRiva, A.; Wang, M.; Engelhard, M. H.; Kovarik, L.; Datye, A. K.; Wang, Y. Activation of surface lattice oxygen in single-atom Pt/CeO₂ for low-temperature CO oxidation. *Science* **2017**, *358* (6369), 1419.
- (21) Liu, L.; Corma, A. Metal Catalysts for Heterogeneous Catalysis: From Single Atoms to Nanoclusters and Nanoparticles. *Chem. Rev.* **2018**, just accepted.
- (22) Pereira-Hernández, X. I.; DeLaRiva, A.; Muravev, V.; Kunwar, D.; Xiong, H.; Sudduth, B.; Engelhard, M.; Kovarik, L.; Hensen, E. J. M.; Wang, Y.; Datye, A. K. Tuning Pt-CeO₂ interactions by high-temperature vapor-phase synthesis for improved reducibility of lattice oxygen. *Nat. Commun.* **2019**, *10* (1), 1358.
- (23) Wang, H.; Liu, J.-X.; Allard, L. F.; Lee, S.; Liu, J.; Li, H.; Wang, J.; Wang, J.; Oh, S. H.; Li, W. Surpassing the single-atom catalytic activity limit through paired Pt-O-Pt ensemble built from isolated Pt 1 atoms. *Nat. Commun.* **2019**, *10* (1), 1-12.
- (24) Engel, T.; Ertl, G. Elementary Steps in the Catalytic Oxidation of Carbon Monoxide on Platinum Metals. In *Advances in Catalysis*, Eley, D. D.; Pines, H.; Weez, P. B., Eds. Academic Press: 1979; Vol. 28, pp 1-78.
- (25) Voltz, S. E.; Morgan, C. R.; Liederman, D.; Jacob, S. M. Kinetic Study of Carbon Monoxide and Propylene Oxidation on Platinum Catalysts. *Product R&D* **1973**, *12* (4), 294-301.
- (26) Langmuir, I. The mechanism of the catalytic action of platinum in the reactions $2\text{CO} + \text{O}_2 = 2\text{CO}_2$ and $2\text{H}_2 + \text{O}_2 = 2\text{H}_2\text{O}$. *Trans. Faraday Society* **1922**, *17* (0), 621-654.
- (27) Vogel, D.; Spiel, C.; Suchorski, Y.; Trincherro, A.; Schlögl, R.; Grönbeck, H.; Rupprechter, G. Local Catalytic Ignition during CO Oxidation on Low-Index Pt and Pd Surfaces: A Combined PEEM, MS, and DFT Study. *Angew. Chem. Int. Ed.* **2012**, *51* (40), 10041-10044.
- (28) Singh, J.; Alayon, E. M. C.; Tromp, M.; Safonova, O. V.; Glatzel, P.; Nachttegaal, M.; Frahm, R.; van Bokhoven, J. A. Generating Highly Active Partially Oxidized Platinum during Oxidation of Carbon Monoxide over Pt/Al₂O₃: In Situ, Time-Resolved, and High-Energy-Resolution X-Ray Absorption Spectroscopy. *Angew. Chem. Int. Ed.* **2008**, *47* (48), 9260-9264.
- (29) Newton, M. Time Resolved Operando X-ray Techniques in Catalysis, a Case Study: CO Oxidation by O₂ over Pt Surfaces and Alumina Supported Pt Catalysts. *Catalysts* **2017**, *7* (2), 58.
- (30) Grunwaldt, J.-D.; Wagner, J. B.; Dunin-Borkowski, R. E. Imaging Catalysts at Work: A Hierarchical Approach from the Macro- to the Meso- and Nano-scale. *ChemCatChem* **2013**, *5* (1), 62-80.
- (31) Weckhuysen, B. M. Chemical Imaging of Spatial Heterogeneities in Catalytic Solids at Different Length and Time Scales. *Angew. Chem. Int. Ed.* **2009**, *48* (27), 4910-4943.
- (32) Gänzler, A. M.; Casapu, M.; Boubnov, A.; Müller, O.; Conrad, S.; Lichtenberg, H.; Frahm, R.; Grunwaldt, J.-D. Operando spatially and time-resolved X-ray absorption spectroscopy and infrared thermography during oscillatory CO oxidation. *J. Catal.* **2015**, *328*, 216-224.
- (33) Chan, D.; Tischer, S.; Heck, J.; Diehm, C.; Deutschmann, O. Correlation between catalytic activity and catalytic surface area of a Pt/Al₂O₃ DOC: An experimental and microkinetic modeling study. *Appl. Catal. B.* **2014**, *156-157*, 153-165.
- (34) Zellner, A.; Suntz, R.; Deutschmann, O. Two-Dimensional Spatial Resolution of Concentration Profiles in Catalytic Reactors by Planar Laser-Induced Fluorescence: NO Reduction over Diesel Oxidation Catalysts. *Angew. Chem. Int. Ed.* **2015**, *54* (9), 2653-2655.
- (35) Portela, R.; Perez-Ferreras, S.; Serrano-Lotina, A.; Bañares, M. A. Engineering operando methodology: Understanding catalysis in time and space. *Front Chem Sci Eng.* **2018**, *12* (3), 509-536.
- (36) Glatzel, P.; Weng, T.-C.; Kvashnina, K.; Swarbrick, J.; Sikora, M.; Gallo, E.; Smolentsev, N.; Mori, R. A. Reflections on hard X-ray photon-in/photon-out spectroscopy for electronic structure studies. *J. Electron. Spectrosc. Relat. Phenom.* **2013**, *188*, 17-25.
- (37) Bauer, M. HERFD-XAS and valence-to-core-XES: new tools to push the limits in research with hard X-rays? *Phys. Chem. Chem. Phys.* **2014**, *16* (27), 13827-13837.
- (38) Günter, T.; Carvalho, H. W. P.; Doronkin, D. E.; Sheppard, T.; Glatzel, P.; Atkins, A. J.; Rudolph, J.; Jacob, C. R.; Casapu, M.; Grunwaldt, J.-D. Structural snapshots of the SCR reaction mechanism on Cu-SSZ-13. *Chem. Commun.* **2015**, *51* (44), 9227-9230.
- (39) Merte, L. R.; Behafarid, F.; Miller, D. J.; Friebel, D.; Cho, S.; Mbuga, F.; Sokaras, D.; Alonso-Mori, R.; Weng, T.-C.; Nordlund, D.; Nilsson, A.; Roldan Cuenya, B. Electrochemical Oxidation of Size-Selected Pt Nanoparticles Studied Using in Situ High-Energy-Resolution X-ray Absorption Spectroscopy. *ACS Catal.* **2012**, *2* (11), 2371-2376.
- (40) Frenkel, A. I.; Small, M. W.; Smith, J. G.; Nuzzo, R. G.; Kvashnina, K. O.; Tromp, M. An in Situ Study of Bond Strains in 1 nm Pt Catalysts and Their Sensitivities to Cluster-Support and Cluster-Adsorbate Interactions. *J. Phys. Chem. C* **2013**, *117* (44), 23286-23294.
- (41) Gorczyca, A.; Moizan, V.; Chizallet, C.; Proux, O.; Del Net, W.; Lahera, E.; Hazemann, J.-L.; Raybaud, P.; Joly, Y. Monitoring Morphology and Hydrogen Coverage of Nanometric Pt/γ-Al₂O₃ Particles by In Situ HERFD-XANES and Quantum Simulations. *Angew. Chem. Int. Ed.* **2014**, *53* (46), 12426-12429.
- (42) Safonova, O. V.; Tromp, M.; van Bokhoven, J. A.; de Groot, F. M. F.; Evans, J.; Glatzel, P. Identification of CO Adsorption Sites in Supported Pt Catalysts Using High-Energy-Resolution Fluorescence Detection X-ray Spectroscopy. *The Journal of Physical Chemistry B* **2006**, *110* (33), 16162-16164.
- (43) Ding, K.; Gulec, A.; Johnson, A. M.; Schweitzer, N. M.; Stucky, G. D.; Marks, L. D.; Stair, P. C. Identification of active sites in CO oxidation and water-gas shift over supported Pt catalysts. *Science* **2015**, *350* (6257), 189.
- (44) Aleksandrov, H. A.; Neyman, K. M.; Hadjiivanov, K. I.; Vayssilov, G. N. Can the state of platinum species be unambiguously determined by the stretching frequency of an adsorbed CO probe molecule? *Phys. Chem. Chem. Phys.* **2016**, *18* (32), 22108-22121.
- (45) Bordiga, S.; Groppo, E.; Agostini, G.; van Bokhoven, J. A.; Lamberti, C. Reactivity of Surface Species in Heterogeneous Catalysts Probed by In Situ X-ray Absorption Techniques. *Chem. Rev.* **2013**, *113* (3), 1736-1850.
- (46) Manyar, H. G.; Morgan, R.; Morgan, K.; Yang, B.; Hu, P.; Szlachetko, J.; Sá, J.; Hardacre, C. High energy resolution fluorescence detection XANES – an in situ method to study the interaction of adsorbed molecules with metal catalysts in the liquid phase. *Catal. Sci. Technol.* **2013**, *3* (6), 1497-1500.
- (47) Boubnov, A.; Carvalho, H. W. P.; Doronkin, D. E.; Günter, T.; Gallo, E.; Atkins, A. J.; Jacob, C. R.; Grunwaldt, J.-D. Selective Catalytic Reduction of NO over Fe-ZSM-5: Mechanistic Insights by Operando HERFD-XANES and Valence-to-Core X-ray Emission Spectroscopy. *J. Am. Chem. Soc.* **2014**, *136* (37), 13006-13015.
- (48) Zhou, Y.; Doronkin, D. E.; Zhao, Z.; Plessow, P. N.; Jelic, J.; Detlefs, B.; Pruessmann, T.; Studt, F.; Grunwaldt, J.-D. Photothermal Catalysis over Nonplasmonic Pt/TiO₂ Studied by Operando HERFD-XANES, Resonant XES, and DRIFTS. *ACS Catal.* **2018**, *8* (12), 11398-11406.
- (49) Iglesias-Juez, A.; Beale, A. M.; Maaijen, K.; Weng, T. C.; Glatzel, P.; Weckhuysen, B. M. A combined in situ time-resolved UV-Vis, Raman and high-energy resolution X-ray absorption spectroscopy study on the deactivation behavior of Pt and PtSn propane dehydrogenation catalysts under industrial reaction conditions. *J. Catal.* **2010**, *276* (2), 268-279.

- (50) Urakawa, A.; Baiker, A. Space-Resolved Profiling Relevant in Heterogeneous Catalysis. *Top. Catal.* **2009**, *52* (10), 1312-1322.
- (51) Morgan, K.; Toutou, J.; Choi, J.-S.; Coney, C.; Hardacre, C.; Pihl, J. A.; Stere, C. E.; Kim, M.-Y.; Stewart, C.; Goguet, A.; Partridge, W. P. Evolution and Enabling Capabilities of Spatially Resolved Techniques for the Characterization of Heterogeneously Catalyzed Reactions. *ACS Catal.* **2016**, *6* (2), 1356-1381.
- (52) Stewart, C.; Gibson, E. K.; Morgan, K.; Cibir, G.; Dent, A. J.; Hardacre, C.; Kondratenko, E. V.; Kondratenko, V. A.; McManus, C.; Rogers, S.; Stere, C. E.; Chansai, S.; Wang, Y.-C.; Haigh, S. J.; Wells, P. P.; Goguet, A. Unraveling the H₂ Promotional Effect on Palladium-Catalyzed CO Oxidation Using a Combination of Temporally and Spatially Resolved Investigations. *ACS Catal.* **2018**, *8* (9), 8255-8262.
- (53) Urakawa, A.; Maeda, N.; Baiker, A. Space- and Time-Resolved Combined DRIFT and Raman Spectroscopy: Monitoring Dynamic Surface and Bulk Processes during NOx Storage Reduction. *Angew. Chem.* **2008**, *120* (48), 9396-9399.
- (54) Hannemann, S.; Grunwaldt, J.-D.; van Vegten, N.; Baiker, A.; Boye, P.; Schroer, C. G. Distinct spatial changes of the catalyst structure inside a fixed-bed microreactor during the partial oxidation of methane over Rh/Al₂O₃. *Catal. Today* **2007**, *126* (1), 54-63.
- (55) Doronkin, D. E.; Casapu, M.; Günter, T.; Müller, O.; Frahm, R.; Grunwaldt, J.-D. Operando Spatially- and Time-Resolved XAS Study on Zeolite Catalysts for Selective Catalytic Reduction of NOx by NH₃. *J. Phys. Chem. C* **2014**, *118* (19), 10204-10212.
- (56) Dixon, A. G.; Deutschmann, O. *Spatially Resolved Operando Measurements in Heterogeneous Catalytic Reactors*. Elsevier: London, 2017; Vol. 50.
- (57) Hettel, M.; Diehm, C.; Torkashvand, B.; Deutschmann, O. Critical evaluation of in situ probe techniques for catalytic honeycomb monoliths. *Catal. Today* **2013**, *216* (Supplement C), 2-10.
- (58) Partridge, W. P.; Storey, J. M. E.; Lewis, S. A.; Smithwick, R. W.; DeVault, G. L.; Cunningham, M. J.; Currier, N. W.; Yonushonis, T. M. Time-Resolved Measurements of Emission Transients By Mass Spectrometry. *SAE Technical Papers* **2000**, 2000-01-2952.
- (59) Horn, R.; Degenstein, N. J.; Williams, K. A.; Schmidt, L. D. Spatial and temporal profiles in millisecond partial oxidation processes. *Catal. Lett.* **2006**, *110* (3), 169-178.
- (60) Sa, J.; Fernandes, D. L. A.; Aiouache, F.; Goguet, A.; Hardacre, C.; Lundie, D.; Naeem, W.; Partridge, W. P.; Stere, C. SpaciMS: spatial and temporal operando resolution of reactions within catalytic monoliths. *Analyst* **2010**, *135* (9), 2260-2272.
- (61) Brunauer, S.; Emmett, P. H.; Teller, E. Adsorption of Gases in Multimolecular Layers. *J. Am. Chem. Soc.* **1938**, *60* (2), 309-319.
- (62) Serre, C.; Garin, F.; Belot, G.; Maire, G. Reactivity of Pt/Al₂O₃ and Pt-CeO₂/Al₂O₃ Catalysts for the Oxidation of Carbon Monoxide by Oxygen: II. Influence of the Pretreatment Step on the Oxidation Mechanism. *J. Catal.* **1993**, *141* (1), 9-20.
- (63) Gatla, S.; Aubert, D.; Agostini, G.; Mathon, O.; Pascarelli, S.; Lunkenbein, T.; Willinger, M. G.; Kaper, H. Room-Temperature CO Oxidation Catalyst: Low-Temperature Metal-Support Interaction between Platinum Nanoparticles and Nanosized Ceria. *ACS Catal.* **2016**, *6* (9), 6151-6155.
- (64) Gänzler, A. M.; Casapu, M.; Maurer, F.; Störmer, H.; Gerthsen, D.; Ferré, G.; Vernoux, P.; Bornmann, B.; Frahm, R.; Murzin, V.; Nachttegaal, M.; Votsmeier, M.; Grunwaldt, J.-D. Tuning the Pt/CeO₂ Interface by in Situ Variation of the Pt Particle Size. *ACS Catal.* **2018**, *8* (6), 4800-4811.
- (65) Grunwaldt, J. D.; Caravati, M.; Hannemann, S.; Baiker, A. X-ray absorption spectroscopy under reaction conditions: suitability of different reaction cells for combined catalyst characterization and time-resolved studies. *Phys. Chem. Chem. Phys.* **2004**, *6* (11), 3037-3047.
- (66) Zhou, Y.; Doronkin, D. E.; Chen, M.; Wei, S.; Grunwaldt, J.-D. Interplay of Pt and Crystal Facets of TiO₂: CO Oxidation Activity and Operando XAS/DRIFTS Studies. *ACS Catal.* **2016**, *6* (11), 7799-7809.